

# Intracellular Trafficking Botulinum Neurotoxin Light Chain A1 to cleave Plasma Membrane Bound SNAP-25

Alexander Gardner<sup>1\*</sup>, William H Tepp<sup>2</sup>, Marite Bradshaw<sup>2</sup>, Joseph T. Barbieri<sup>1</sup>, and Sabine Pellett<sup>2</sup>

<sup>1</sup>Department of Microbiology and Immunology, Medical College of Wisconsin, 8701 Watertown Plank Rd, Milwaukee, WI 53226, USA.

<sup>2</sup>Department of Bacteriology, University of Wisconsin-Madison, 1550 Linden Dr, Madison, WI 53706, USA.

## Abstract

Botulinum neurotoxins (BoNTs) are among the most potent protein toxins known to humans, yet the intracellular trafficking of BoNT-Light Chain A1 (LC/A1) to its substrate, Synaptosome Associated Protein of 25-kDa (SNAP-25), remains poorly understood. A mouse neuroblastoma-2A (N2A) cell-based assay was used to track the intracellular trafficking of cytosolic EGFP-tagged LC/A1. The results revealed that LC/A1 associates with intracellular vesicles as a function of the LC/A1-N terminus, while plasma membrane binding is facilitated by an internal region of LC/A1 that can target LC/A1 to the plasma membrane from the cytosol. An internal LC/A1 domain, termed the Membrane Localization Domain (MLD), is responsible for the movement of the LC/A1 to the plasma membrane, where the association may be stable or reversible depending on the LC/A subtype. Recent studies have detected the physical trafficking of EGFP-LC/A1 from the cytosol to the intracellular plasma membrane. Thus, in addition to known steps such as host receptor binding and catalysis, the intracellular trafficking of LC to the target substrate may be a critical determinant of BoNT potency. Mechanistic insights into BoNT intracellular trafficking will clarify fundamental aspects of toxin action towards the development of novel therapeutic strategies to mitigate BoNT toxicity.

## Recovery of SNAP-25 after Exposure to BoNT/A

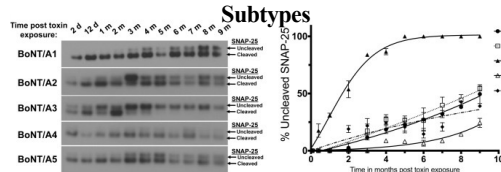


Figure 1

- Left panel. Western Blot cleavage of SNAP-25 from BoNT/A subtypes A1-A5.
- Right panel. Recovery of uncleaved SNAP-25. A1, A2, A4, and A5 had a slow recovery being  $\leq 50\%$  uncleaved SNAP-25 9-months post intoxication. Intoxication with A3 shows rapid recovery to 100% uncleaved SNAP-25 6-months post intoxication.

## Mapping Regions of LC/A which Contribute to Intracellular Localization in Neuro-2A Cells

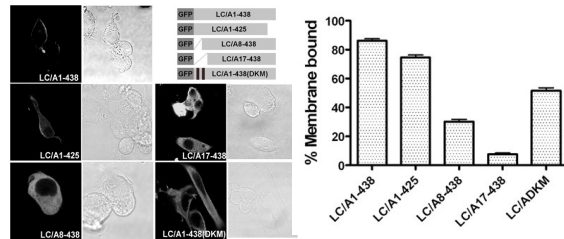


Figure 2

- Left panel. N-terminal (NT) truncations resulted in a larger loss % of membrane localization than both the C-terminal region and double lysine mutant (DKM) control, K6A and K11A.
- Right panel. Subcellular fractionation shows that NT truncations resulted in a larger loss of membrane-bound LC/A1 than both the C-terminal truncations and DKM control for LC/A1.

## Intracellular Localization of BoNT LC/A Subtypes

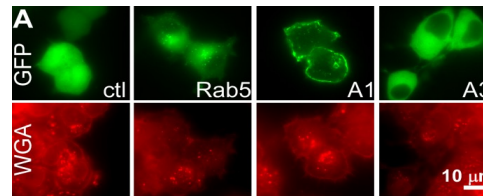
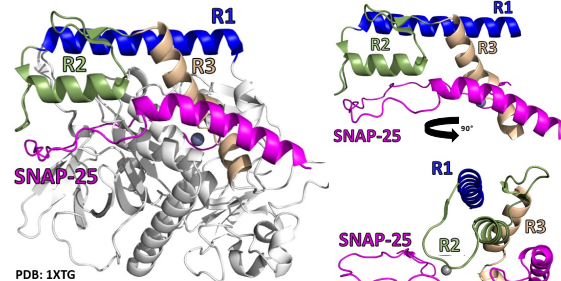


Figure adapted from Pellett S. et al. mBio. 2018

Figure 3

- Figure 3A. GFP-LC/A1 and GFP-LC/A3 are membrane and cytosolic in localization, respectively. GFP and Rab5 were utilized as controls for expression and an early endosome marker, respectively.
- Bottom row: Wheat Germ Agglutinin (WGA) is a membrane stain.

## Structural Model of BoNT LC/A1 R1, R2, and R3



PDB: 1XTG

Figure 4

Figure adapted from Gardner S. et al. JMS. 2022

- Figure 4. A Co-crystal structure of LC/A1 (PDB: 3XTG), R1 (an  $\alpha$ -helix, residues 275-300), R2 (a loop,  $\alpha$ -helix, loop, residues 302-334), and R3 (an  $\alpha$ -helix, turn,  $\alpha$ -helix, residues 335-357) and SNAP-25 (an  $\alpha$ -helix and loop, residues 141-206).

## Chimera Construct Names and Mapping

LC/A3V(A1-LHD) Chimeras*	Designation	Chimera Schematic
EGFP-LC/A3V(A1 275-300)	LC/A3V(R1)	GFP LC/A3V R1
EGFP-LC/A3V(A1 302-334)	LC/A3V(R2)	GFP LC/A3V R2
EGFP-LC/A3V(A1 335-357)	LC/A3V(R3)	GFP LC/A3V R3
EGFP-LC/A3V(A1 275-334)	LC/A3V(R1:R2) [MLD]	GFP LC/A3V R1 R2
EGFP-LC/A3V(A1 302-357)	LC/A3V(R2:R3)	GFP LC/A3V R2 R3
EGFP-LC/A3V(A1 275-300, 335-357)	LC/A3V(R1:R3)	GFP LC/A3V R1 R2 R3
EGFP-LC/A3V (A1 268-357)	LC/A3V(LHD)	GFP LC/A3V R1 R2 R3

\* Chimeras utilized LC/A3V [residues 1-446] as a platform exchanging regions from LC/A1 LHD

<sup>1</sup> MLD: Membrane localization domain residues 275-334 from LC/A1

<sup>2</sup> LHD: low homology domain residues 268-357 from LC/A1

Figure 5

- GFP-LC/A3 chimeras were designed to see if the which regions from the LHD from LC/A1 are necessary for localization of LC/A3V to the inner leaflet of the plasma membrane.
- Controls are EGFP, EGFP-LC/A1, and EGFP-LC/A3V for expression, membrane and cytosolic localization, respectively.

## Intracellular Localization of GFP-LC/A3V (A1- LHD) chimeras

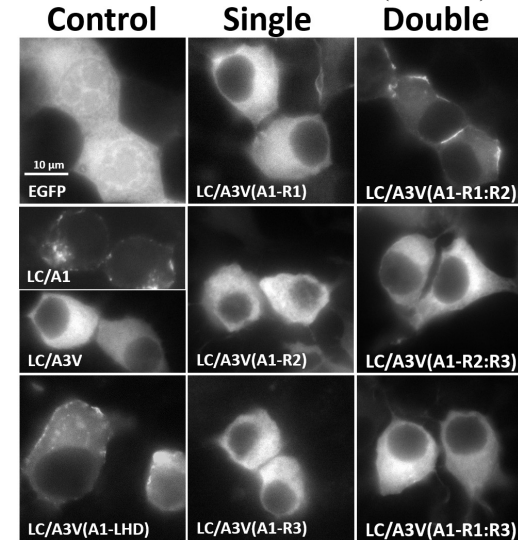


Figure adapted from Gardner S. et al. JMS. 2022

Figure 6

- Figure 6. At steady-state, individual A1 R regions did not transition cytosolic LC/A3V from the cytosol to the plasma membrane.
- Dual-A1 R region chimera targeted LC/A3V(R1:R2) to the plasma membrane, while LC/A3V(R2:R3) and LC/A3V(R1:R3) were expressed in the cytosol.

## Intracellular Localization of BoNT/A subtypes- LC/A1, LC/A3LM, and LC/A3V

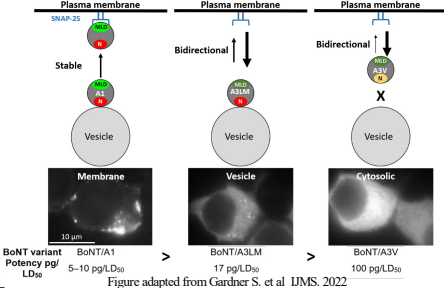


Figure adapted from Gardner S. et al. JMS. 2022

Figure 7

- Figure 7. Immunofluorescent data supports the sequential step model for the intracellular localization of LC/A1 described in, where the N terminus of LC/A1 targets LC anterograde trafficking on vesicles, and the MLD targets LC/A1 to stably co-localize with SNAP-25 on the plasma membrane.
- The intracellular localization has been shown to correlate with localization with membrane (LC/A1) having the highest potency and cytosolic (LC/A3V) having the lowest.